Journal of the Ceramic Society of Japan 122 [1] 29-34 2014 Paper

Preparation and evaluation of ferrite-silica aerogel nanocomposite

Naruhito KATAGIRI,[*,,†] Nobuyasu ADACHI[**] and Toshitaka OTA[**]**

[*]Technology Development Center, Rinnai Corporation, 3–1 Kaechi, Oguchi-cho, Niwa-gun, Aichi 480–0133, Japan
[**]Advanced Ceramics Research Center, Nagoya Institute of Technology, 10–6–29 Asahigaoka, Tajimi, Gifu 507–0071, Japan

The ferrite-silica aerogel nanocomposite prepared by a sol–gel process and a supercritical drying process was investigated from the point of view of new composite material. The ferrite nanoparticles were prepared by a coprecipitation method and added to tetramethylorthosilicate (TMOS) in the range of 0 to 20 mol %. The ferrite-silica wet gel was prepared from TMOS containing ferrite nanoparticles, ethanol, deionized water and NH_3 aq. as a catalyst, and replaced the liquid phase and aged in the ethanol. Then, a hydrophobing treatment was performed in hexamethyldisilazane toluene solution. Finally, the ferrite-silica wet gel was dried in the supercritical carbon dioxide fluid. The obtained ferrite-silica aerogel nanocomposite was evaluated by bulk density, porosity, specific surface area, pore size distribution, SEM and TEM observation, EDS analysis and magnetization measurement by VSM. As a result, even if it added the ferrite, the characteristics of aerogel was held and the magnetic property of the ferrite remained unchanged in the aerogel.

Key-words : Magnetic property, Ferrite, Silica aerogel, Nanocomposite, Sol–gel, Supercritical drying

[Received August 28, 2013; Accepted October 21, 2013]

1. Introduction

Aerogel is a porous material derived from a gel, in which the liquid component of the gel has been replaced with a gas. The main properties of aerogel are an extremely low density ($<200\,mg/cm^3$), a high porosity (>90%), a high specific surface area ($150–1000\,m^2\,g^{-1}$) and a low thermal conductivity ($<0.02\,W/m{\cdot}K$).[1),2)] Thus, aerogel is practically used as carrier and a catalyst.[3)] In addition, it is known unique properties such as transparency and a low refractive index, from the characteristic of the structure. By utilizing these properties, some applications such as a transparent low refractive-index material for Cerenkov detectors, a transparent low density material for collecting cosmic dust etc. has been also put into practical use.[4)]

Usually, an aerogel is prepared by a supercritical drying using carbon dioxide in wet gel obtained by a hydrolysis of metal alkoxide and by a condensation polymerization. As typical aerogels, silica aerogel, alumina aerogel and carbon aerogel are well-known. In addition, some aerogels with functional particles have been studied. For example, an aerogel composed of titania and silica[5)] or the composite of metallic nickel and alumina aerogel[6)] exhibited superior catalytic performance. However, any functional aerogels consisting of a magnetic and dielectric materials have not been prepared due to uncontrollable gelation and lack of variety of their metal alkoxides and their expensive cost etc. In this paper, ferrite-silica aerogel nanocomposites were prepared from a mixture of silica sol and ferrite nanoparticles by a supercritical drying process. This new magnetic aerogel might be applied to electromagnetic wave absorber,[7)] and hyperthermia[8)] etc.

† Corresponding author: N. Katagiri; E-mail: NaruhitoKatagiri@rinnai.co.jp

‡ Preface for this article: DOI http://dx.doi.org/10.2109/jcersj2.122.P1-1

2. Experimental procedure

2.1 Preparation of ferrite nanoparticles

Ferrite nanoparticles were prepared by a coprecipitation method.[9)] Raw materials of $FeCl_3{\cdot}6H_2O$, $NiCl_2{\cdot}6H_2O$ and $ZnCl_2$ (Wako Pure Chem. Ind., Ltd.) were weighed to be $x = 0.1$ in $Ni_xZn_{1-x}Fe_2O_4$ and dissolved by adding distilled water. The solution was adjusted to pH 13 by adding NaOH, and then refluxed at 110°C for 24 h. After cooling, excess NaOH was removed from the precipitation by washing repeatedly with distilled water and ethanol, resulting in ferrite nanoparticles. The obtained ferrite nanoparticles were used as ethanol suspension of about 0.07 g/mL without drying.

Synthesized ferrite nanoparticles were identified by a powder X-ray diffractometer (XRD, Rigaku, RINT1000). The particle size distribution was measured by dynamic light scattering particle size analyzer (Particle Sizing Systems,Nicomp380ZLS). The composition was analyzed by X-ray fluorescence (Rigaku, ZSX100e).

2.2 Preparation of ferrite-silica aerogel nanocomposites

There are many reports on preparation of silica aerogel. In this experiment, the report by Tajiri and Tsuchiya et al. was referred.[2),10)] Used reagents were as follows: tetramethylorthosilicate(TMOS, Tokyo Chem. Ind. Co., Ltd.); 1,1,1,3,3,3-hexamethyldisilazane(Tokyo Chem. Ind. Co., Ltd.); NH_3 aq. (28 mass % aqueous solution, Wako Pure Chem. Ind. Ltd.) and ethanol (Wako Pure Chem. Ind. Ltd.).

First, ferrite nanoparticles were added to TMOS ethanol solution and were mixed for 10 min on a magnetic stirrer. Then the mixture was homogenized for 5 min by ultrasonic wave. Second, deionized water and NH_3 aq. as a catalyst were added in sequence and stirred for 5 min, respectively. The obtained sol was injected

DOI http://dx.doi.org/10.2109/jcersj2.122.29

to a resin mold of $\phi 5 \times 5$ mm and $\phi 20 \times 3$ mm, and aged at 50°C for 2 h in an ethanol. As a result, the sol became to a wet gel. This processing was performed in an ultrasonic wave container in order to avoid a sedimentation of ferrite particles. The obtained wet gel was refluxed at 110°C for 24 h in 1.3 mol/L hexamethyldisilazane toluene solution for a hydrophobic treatment. After cooling, the toluene inside the wet gel was again replaced by an ethanol. Then, the wet gel was treated by the supercritical drying using carbon dioxide, resulting in ferrite-silica aerogel nanocomposites.

2.3 Evaluation of ferrite-silica aerogel nanocomposites

The bulk density and the porosity were calculated from the measurement of size and weight. The specific surface area was measured by BET method. The pore size distribution was measured by BJH method from volumetric nitrogen gas adsorption (Bell Japan, Inc., BELSORP-max) for a mesopore region, and by mercury intrusion porosimeter (Thermo Fisher Scientific Inc., PASCAL140/240) for a macropore region. The microstructure was observed by a field emission scanning electron microscope (FE-SEM, JEOL Ltd., JSM-7000F) and a transmission electron microscope (TEM, JEOL Ltd., JEM-2100). The composition was analyzed by an energy dispersive X-ray spectrometry (EDS, JEOL Ltd., JED-2300F and EX-230 ** BU). The magnetization measurement was performed by a vibrating sample magnetometer (VSM, Toei Ind. Co., Ltd.,VSM-5).

3. Results and discussion

3.1 Ferrite nanoparticles

Figure 1 shows the powder X-ray diffraction pattern measurement of the ferrite nanoparticles. The peaks was identified as $(Ni,Zn)Fe_2O_4$. By using a diffraction peak of $2\theta = 35°$, the crystallite size was calculated from Scherrer's equation(1).

$$L = K\lambda/(\beta \cos\theta), \quad (1)$$

where L is a crystallite size, λ is a wavelength of X-ray, β is a half width, K is a constant (0.9 in this run). As a result, the crystallite size was estimated to be 14 nm.

Figure 2 shows the cumulative particle size distribution of the ferrite nanoparticles. It demonstrated that the ferrite particles was overall nano size since d_{90} was 128 nm. The average diameter (d_{50}) was 65 nm, which was larger than the value calculated from Scherrer's equation. Therefore, it was considered that the ferrite nanoparticles somewhat agglomerated.

Table 1 summarizes the composition analysis of the ferrite. It demonstrated that $Ni_{0.1}Zn_{0.9}Fe_2O_4$ was prepared as designed.

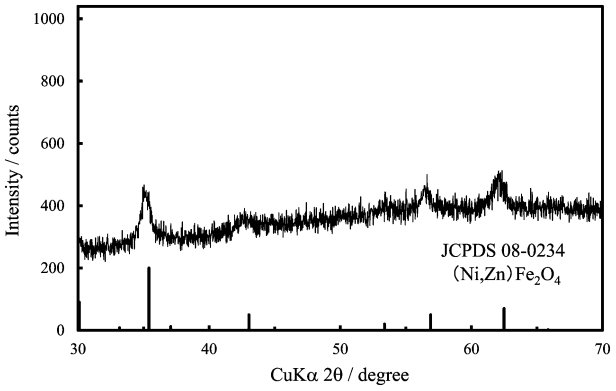

Fig. 1. XRD pattern of ferrite nanoparticles.

3.2 Preparation of ferrite-silica aerogel nanocomposite

A condensation polymerization of TMOS proceeded by the addition of both H_2O for the hydrolysis and NH_3 aq. as a catalyst to form a silica gel. The time required for gelation was significantly affected by the concentration of TMOS in ethanol solution. The gelation time increased with increasing in ethanol/TMOS molar ratio. When the molar ratio was in the range from 6 to 11, TMOS gelled within 1 h, which was a preferable time for an experimental processing. Since the ferrite was dispersed in ethanol from the start, the content of ferrite was automatically fixed. **Figure 3** shows the relationship between ethanol/TMOS molar ratio, gelation time and maximum ferrite content. In this run, ethanol/TMOS molar ratio = 11 was selected in order to prepare a sample containing 20 mol % of ferrite.

The liquid phase substitution and aging were important process in order to remove catalyst and water remaining in the wet gel, and to accelerate the condensation polymerization, respectively. **Figure 4** shows the change of the amount of residual water in the wet gel after repeating substitution. By substituting 5 times, the residual water in the wet gel became to 10% or less and since then there was no significant decrease of residual water even if the substituting was repeated furthermore.

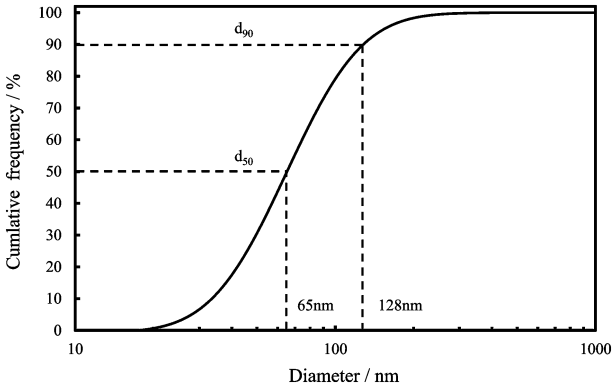

Fig. 2. Particle size distribution of ferrite nanoparticles.

Table 1. (a) Composition analytical result of ferrite (wt %)

Fe_2O_3	ZnO	NiO	SiO_2 and others
65.0	29.6	3.3	2.2

(b) Moler ratio conversion

Fe_2O_3	ZnO	NiO
1.0	0.9	0.1

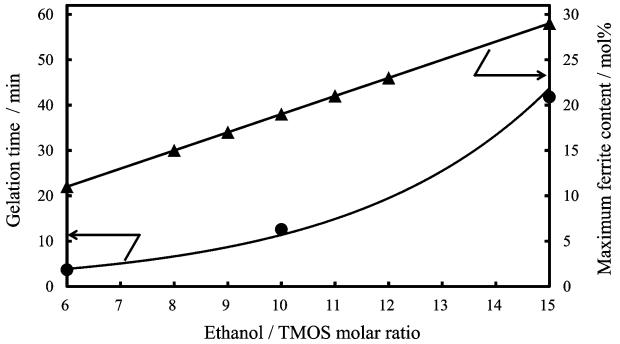

Fig. 3. Relationship between ethanol/TMOS molar ratio, gelation time and maximum ferrite content.

Table 2. Trial by supercritical drying process

State of CO_2	Temperature pressure	Number of substitution	Treatment time	After treatment
1) liquid	room temp. 9 MPa	1	3 h	shrinking cracking
2) liquid	room temp. 9 MPa	5	6 h	shrinking cracking
3) supercritical	40°C 9 MPa	1	24 h	shrinking cracking
4) supercritical	40°C 9 MPa	5	6 h	unchange

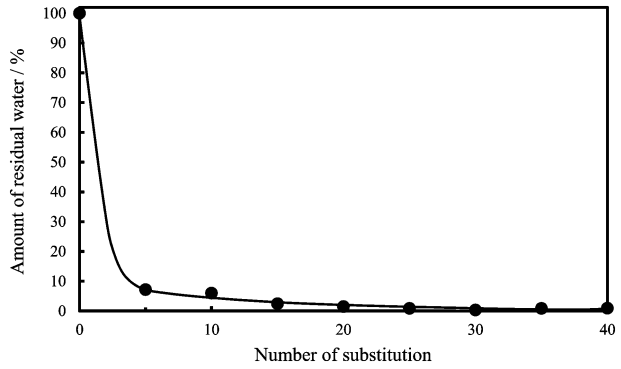

Fig. 4. Changes in the amount of residual water in the wet gel by the number of substitution.

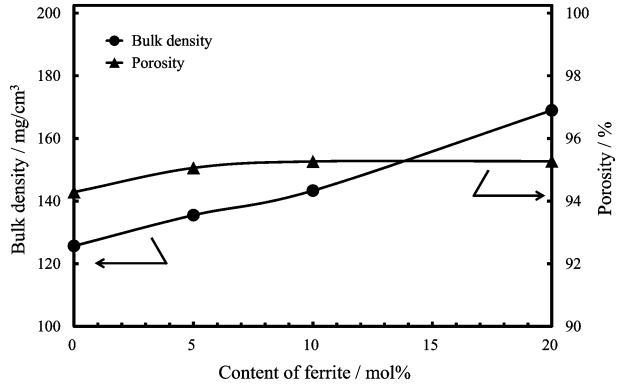

Fig. 5. Bulk density and porosity of ferrite-silica aerogel nanocomposites.

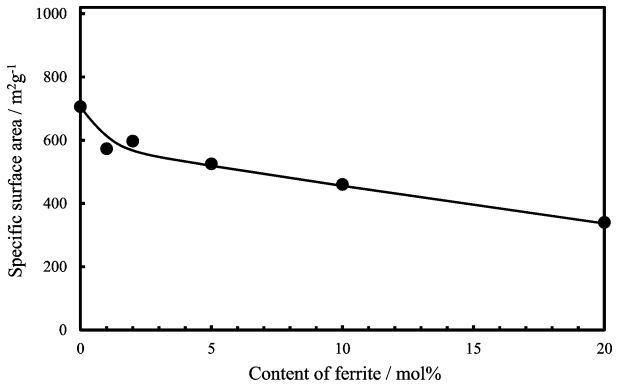

Fig. 6. Specific surface area of ferrite-silica aerogel nanocomposites.

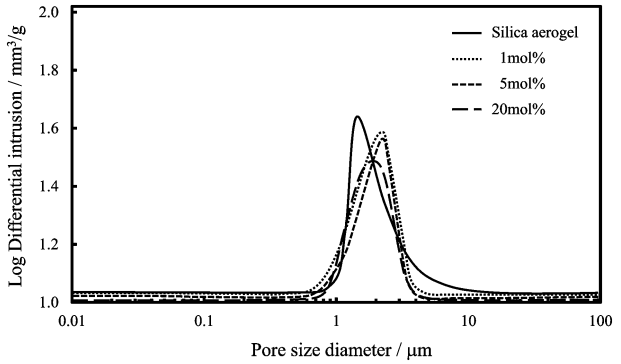

Fig. 7. Pore size distribution of ferrite-silica aerogel nanocomposites in the macropore region.

The supercritical drying process was a key process in this run. **Table 2** summarizes various trial.[2),11),12)] In the process of 1) and 2), where liquid CO_2 was used as a substitution medium, the obtained samples shrink and/or cracked with the surface tension of the ethanol which remained inside the wet gel, even if the substitution was repeated several times. When supercritical CO_2 was used as a substitution medium, the ethanol inside the wet gel was not completely replaced by only 1 time of substitution, even if the treatment was continued for long time as shown in process of 3). However, in the process of 4), where the substitution was repeated 5 times, the ethanol was completely replaced by supercritical CO_2. Therefore, since there was not any surface tension at the time of dryness, a transparent aerogel was obtained without shrinking and cracking.

3.3 Characterization of ferrite-silica aerogel nanocomposites

Figure 5 shows the bulk density and the porosity of the ferrite-silica aerogel nanocomposites. The bulk density was increased with increasing in the content of ferrite, since the density of ferrite was larger than that of silica. On the other hand, the porosity hardly changed.

Figure 6 shows the specific surface area of the ferrite-silica aerogel nanocomposites. The specific surface area was about 700 $m^2 g^{-1}$ for the silica aerogel. On the other hand, it decreased with increasing in content of ferrite to become to 340 $m^2 g^{-1}$ for 20 mol % for the ferrite-silica aerogel nanocomposites. In regard to the pore size distribution, the median size of macropore for both the silica aerogel and the nanocomposites were around 2 μm as shown in **Fig. 7**. In addition, the median size of mesopore was 14 nm for silica aerogel and shifted to approximately 30 nm with increasing in the content of ferrite as shown in **Fig. 8**. Therefore, it was estimated that the porosity was affected mainly by macropores, while the specific surface area was affected mainly by mesopores. Anyway, it was found that the ferrite-silica aerogel nanocomposites held characteristics of aerogel.

3.4 Microstructure of ferrite-silica aerogel nanocomposites

Figure 9 shows SEM images of the silica aerogel and the ferrite-silica aerogel nanocomposite added 1 mol % of ferrite. Both the silica aerogel and the nanocomposite consisted of particles of approximately 50 nm, which three-dimensionally connected together to form a skeletal network structure. It looked just

as if chains of particles surrounded the bubbles of air. Then, the size of bubble, that is a macropore, was measured by using the intercept method.[13] As a result, the pore size was estimated to 0.9 µm for the silica aerogel and 1.2 µm for the nanocomposite. These sizes accorded with it was thought that the pore sizes shown in Fig. 7. In addition, the ferrite particles existed homogeneously in the nanocomposite as shown in Figs. 9(e) and 9(f).

Figure 10 shows TEM images, element analysis and electron diffraction of the silica aerogel and the ferrite-silica aerogel nanocomposite added 1 mol % of ferrite. Both the silica aerogel and the nanocomposite consisted of particles of 2 to 3 nm, which three-dimensionally connected together to form a skeletal network structure. It was a similar structure as shown in Fig. 9, but

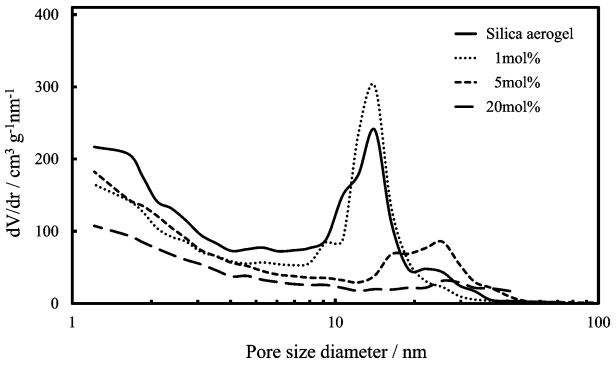

Fig. 8. Pore size distribution of ferrite-silica aerogel nanocomposites in the mesopore region.

on a scale of one to ten. This is to say, the skeletal network structure was fractally held from macropore to mesopore. The pore size surrounded by nanoparticles in the skeletal network structure was about 10 to 20 nm, which was in good agreement with the pore size shown in Fig. 8. The ferrite particles ware identified by the element analysis and the electron diffraction as shown Fig. 10(c), where elements consisting of ferrite were detected for larger particles of about 15 nm, and the electron diffraction demonstrated to be spots for the ferrite crystal. In addition, the size of 15 nm was in good agreement with the crystallite size calculated from Scherrer's equation. However, the dispersion of the ferrite particles was not so good, since some particles aggregated as shown in Figs. 10(b) and 10(c). The aggregated ferrite particles were surrounded by silica nanoparticles, where the skeletal network structure was somewhat broken. Therefore, it was considered that such a heterogeneity of skeletal network structure caused the increase in pore size in the mesopore region, resulting in the decrease in the specific surface area.

3.5 Magnetic property of ferrite-silica aerogel nanocomposites

Figure 11 shows the magnetization curves of the ferrite powder and the ferrite-silica aerogel nanocomposites measured by VSM. As a matter of course, the magnetic susceptibility of the ferrite-silica aerogel nanocomposites increased with increasing in content of ferrite. However, as shown in **Fig. 12**, the magnetic susceptibility per 1 g of ferrite contained in the nanocomposites was equal to the value measured for the ferrite powder only.

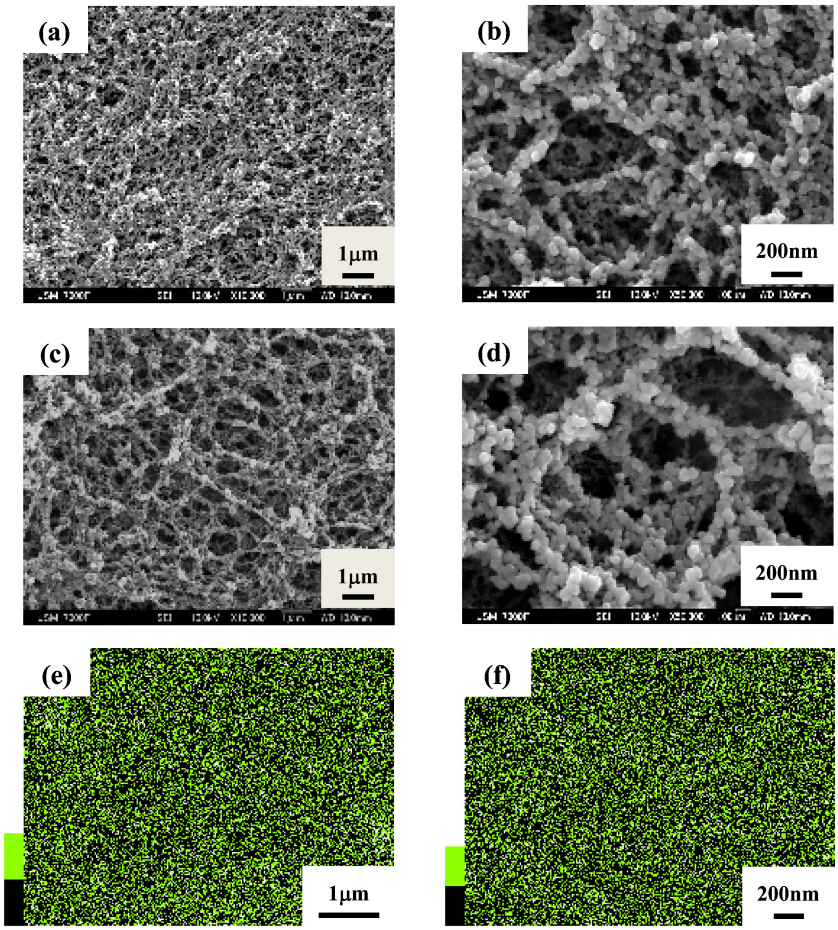

Fig. 9. SEM images of silica aerogel [(a) and (b)] and ferrite-silica aerogel nanocomposite added 1 mol % of ferrite [(c) and (d)], and Fe mapping of nanocomposite [(e) and (f)].

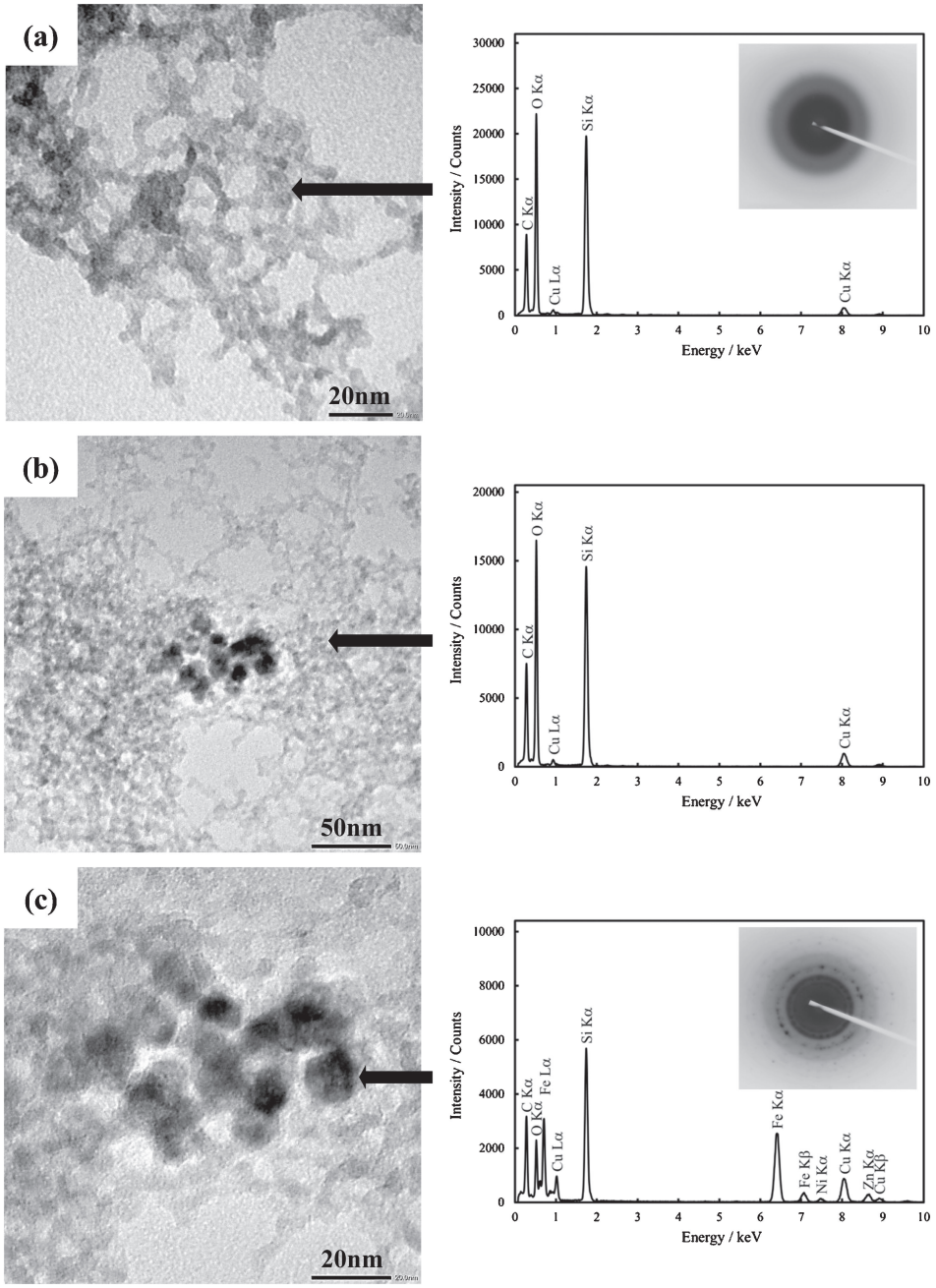

Fig. 10. TEM images, element analysis and electron diffraction of silica aerogel (a) and ferrite-silica aerogel nanocomposite added 1 mol % of ferrite [(b) and (c)].

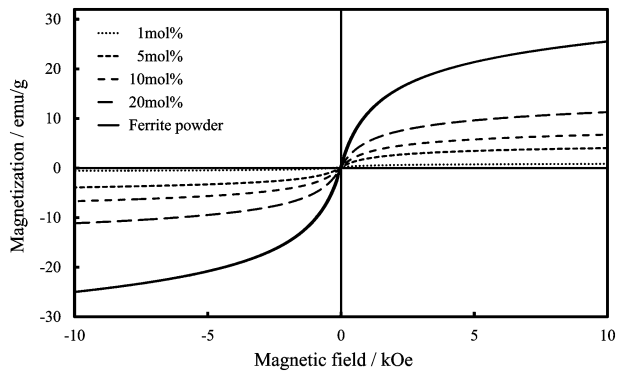

Fig. 11. Magnetization curves of ferrite-silica aerogel nanocomposites and ferrite powder.

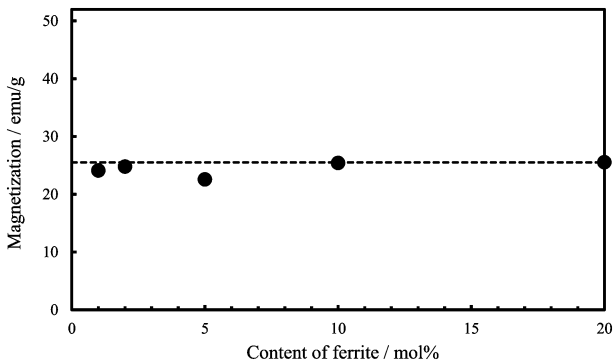

Fig. 12. Mamagnetic susceptibility per 1 g of ferrite in ferrite-silica aerogel nanocomposites at 10 kOe. (dotted line: value of ferrite powder)

Therefore, it was considered that the magnetic property of ferrite was entirely held in the ferrite-silica aerogel nanocomposites.

4. Conclusion

An aerogel with a magnetic property was prepared by a supercritical drying process from a mixture of ferrite nanoparticles and silica sol. The obtained ferrite-silica aerogel nanocomposites had three-dimensional skeletal network structure with macropores of about 2 μm and mesopores of 10 to 30 nm. The porosity was about 95%. The specific surface area changed from 700 to 340 $m^2 g^{-1}$ with increasing in content of ferrite. The ferrite nanoparticles somewhat aggregated due to a poor dispersion. However, the characteristics as a so-called aerogel was held in the ferrite-silica aerogel nanocomposites. In addition, a magnetic property of the ferrite remained unchanged in the aerogel nanocomposites. Therefore, it was expected that many kinds of functional aerogels could be prepared by this way.

References

1) Aerogel-Wikipedia, http//ja.wikipedia.org/wiki/ (accessed 2009-12-18).
2) K.Tajiri, Doctor Thesis, Nagoya Institute of Technology (2002).
3) C. T. Wang and R. J. Willey, *J. Non-Cryst. Solids*, **225**, 173–177 (1998).
4) M. Tabata, Master Thesis, The University of Chiba (2006) http://www.ppl.phys.chiba-u.jp/∼makoto/publication/master-thesis_M.Tabata.pdf (accessed 2013-10-7).
5) L. Luo, A. T. Cooper and M. Fan, *J. Hazard. Mater.*, **161**, 175–182 (2009).
6) T. Ozaki, T. Horiuchi, T. Sugiyama, K. Suzuki and T. Mori, National Industrial Research Institute of Nagoya, Japan Patent, P3136336 (2000).
7) Ferrite Powders for High Frequency Radio Wave Absorber, *JFE Technical Report*, No.26, 77–79(2010).
8) H. Matuski, K. Sato and K. Murakami, *IEEJ Transactions on Fundamentals and Materials*, **9**, 811–815 (1991).
9) Y. Harada, Master Thesis, The University of Mie (2007) http://miuse.mie-u.ac.jp/bitstream/10076/8987/1/2006T038.pdf (accessed 2012-2-14).
10) T. Tuchiya and K. Nishio, Synthesis of the ceramics by a sol gel process, http://www.hst.titech.ac.jp/∼meb/Ceramics/hybrid/hybrid.htm (accessed 2010-9-17).
11) K. Sonoda, M. Yokoyama, H. Yokogawa and K. Tubaki, Panasonic ElectricWorks, Japan Patent, P3339393 (2002).
12) H. Namatsu, Nippon Telegraph and Telephone, Japan Patent, P3492528 (2003).
13) J. C. Wurst and J. A. Nelson, *J. Am. Ceram. Soc. Discussions and Notes*, **2**, 109 (1972).